Construction and Building Materials 278 (2021) 122250

Contents lists available at ScienceDirect

Construction and Building Materials

journal homepage: www.elsevier.com/locate/conbuildmat

Review

Review of moisture measurements in civil engineering with ground penetrating radar – Applied methods and signal features

Tim Klewe [a,*], Christoph Strangfeld [a], Sabine Kruschwitz [a,b]

[a] Bundesanstalt für Materialforschung und -prüfung, Unter den Eichen 87, 12205 Berlin, Germany
[b] Technische Universität Berlin, Straße des 17. Juni 135, 10623 Berlin, Germany

HIGHLIGHTS

- A detailed literature review is given regarding the different signal features for moisture measurement in civil engineering.
- Applied signal features can be grouped into amplitude, time and frequency features.
- An Overview of applied signal features is presented regarding their group, wave type, preceding survey method and use for moisture content estimation.
- Quantitative estimations deliver good results in laboratory conditions, on site measurements underly a lot of uncertainties and mostly allow only qualitative estimations.
- Most reviewed publications consider only one signal feature, thus future approaches may include multiple features for further development.

ARTICLE INFO

Article history:
Received 7 July 2020
Received in revised form 15 December 2020
Accepted 3 January 2021

Keywords:
Ground Penetrating Radar (GPR)
Moisture
Civil engineering
Signal features

ABSTRACT

When applying Ground Penetrating Radar (GPR) to assess the moisture content of building materials, different medium properties, dimensions, interfaces and other unknown influences may require specific strategies to achieve useful results. Hence, we present an overview of the various approaches to carry out moisture measurements with GPR in civil engineering (CE). We especially focus on the applied signal features such as time, amplitude and frequency features and discuss their limitations. Since the majority of publications rely on one single feature when applying moisture measurements, we also hope to encourage the consideration of approaches that combine different signal features for further developments.

Contents

* Corresponding author.
E-mail address: tim.klewe@bam.de (T. Klewe).

https://doi.org/10.1016/j.conbuildmat.2021.122250
0950-0618/

1. Introduction

In civil engineering (CE), all constructions are facing several types of degradation, which cause expensive costs of repair. Frequently occurring degradations are the migration of chloride ions [1], leading to corrosion [2], alkali-silica reaction [3], mould [4], frost-thaw cycle, micro cracking [5], spalling, salt efflorescence [6], etc. All these degradation processes are promoted by an increased amount of material moisture and affect building materials such as concrete, steel, wood, stones, bricks, and screed [7]. Constructions in the field of transport infrastructure, building constructions, or hydraulic structures are mainly made of reinforced concrete [8]. Therefore, the moisture content in the porous cement matrix of concrete is an important and crucial parameter. However, a reliable and non-destructive investigation of the moisture content is still very complex and challenging, while the costs of repair rise continuously. Especially in the field of building constructions, ageing pipe systems are becoming a high burden for insurance. In 2018, 2.9 billion Euro of damage was caused by piped water, accounting for the largest share (49%) of building insurance claims in Germany [9]. In the event of damage, the accurate determination and localization of water ingress is essential to plan for and perform efficient renovations.

There are various methods to approach this task, ranging from destructive (Darr test, calcium carbide method) to non-destructive procedures (electrical, capacitive, radiometric, thermal and hygromatic) [10,11]. While destructive methods are time and cost intensive, most non-destructive measurements are comparatively easy to perform, however, without the use of complex processing and interpretation procedures, they deliver only qualitative results.

Ground Penetrating Radar (GPR) is a fast and widely used measurement method based on electromagnetic waves. Although Radio Detection And Ranging (Radar) is commonly applied for aircraft and ship detection [12], it is used in many other applications like weather forecasts [13] or collision avoidance in the automotive industry [14]. Apart from that, it recently received attention from a wider audience with its application to prove the existence of water on Mars [15]. Over the last decades, many publications already demonstrated the high sensitivity of GPR for water, especially in geophysics [16,17]. However, also in CE it is increasingly used for nondestructive moisture measurements (e.g. [18–22]).

A variety of publications have shown multiple ways to assess moisture with GPR. Different building materials and inspection purposes require individual methods concerning the antenna configuration or the used frequency. The applied setup as well as the underlying structure highly influence the subsequent interpretation of the recorded data, which is why also numerous signal features have been established. Due to the many possibilities to perform moisture measurements with GPR, this review gives an overview of the various methods and their limitation in the context of CE. It shall serve as a basis for inexperienced readers, as well as for advanced users, to encourage further development. Approaches that combine different features or even methods, like data fusion and machine learning, could also benefit from this overview.

2. Fundamentals of GPR

GPR signals are electromagnetic waves whose dynamic behavior is mathematically expressed by Maxwell's equations [23,24]. The wave propagation in investigated objects is highly dependent on the particular electrical properties of the underlying material. Those properties are described by dielectric permittivity ε, electrical conductivity σ, and magnetic permeability μ.

While an influence of μ is neglectable in the majority of GPR applications, ε and σ are of high importance [25]. A low electrical conductivity σ provides the best conditions for an effective use of GPR since the energy is primarily maintained in low-loss materials. Less attenuation allows signals to penetrate deeper into a given material, which results in a better signal-to-noise ratio for low-lying regions of interest. The velocity of wave propagation in low-loss and nonmagnetic materials can be calculated with Eq. (1) [25,26].

$$v = \frac{c_0}{\sqrt{\varepsilon_r}} \tag{1}$$

As the speed of light c_0 is constant, the wave velocity is a function of the relative permittivity ε_r (with $\varepsilon_r = \frac{\varepsilon}{\varepsilon_0}$ and the electric permittivity in vacuum $\varepsilon_0 = 8.854 \cdot 10^{-6} \frac{As}{Vm}$). The relative permittivity describes the dielectric characteristics of materials and is defined as a complex value, where the real and imaginary part are associated with energy storage and dissipation, respectively [16]. While the real part of most building materials is considered as constant and dominant between 10 MHz and 1000 MHz, the frequency-dependent loss becomes relevant as you get closer to the water relaxation frequency between 10 GHz and 20 GHz [25,27]. According to the popular models of Debye [28] and Cole–Cole [29] this results in a decreasing real part and an increasing imaginary part of ε_r for higher frequencies. Following Eq. 1 smaller real parts of ε_r cause higher velocities. However, this effect is not measurable in common GPR applications on building materials, since the high frequency components of transmitted broadband impulses also experience more attenuation due to an increased imaginary part. The frequency dependent attenuation leads to a shift towards lower frequencies that can be observed with rising water contents (see Section 5.3). Furthermore, the enhanced scattering of higher frequencies on heterogeneities leads to additional damping, which limits the possible penetration depth [30,31].

The real value of ε_r is 1 for air and approximately 81 for pure water in liquid phase. For most of dry soils and building materials ε_r is in the range of 2–9 [26] and increases with a higher water content (e.g. ε_r is 10 to 20 for wet concrete). Due to these significant differences, the water content is considered as the main influence on dielectric properties of building materials, which highly justifies the use of GPR for moisture measurements [32].

A related method that also utilizes the influence of water on the electric permittivity and the resulting attenuation of electromagnetic waves is the application of microwave measurements. A review of the various concepts is presented by Okamura [33].

2.1. Wave propagation and received signals

The occurrence of reflection, refraction, and transmission on boundaries between two different permittivities is an important behavior to describe the propagation of electromagnetic waves.

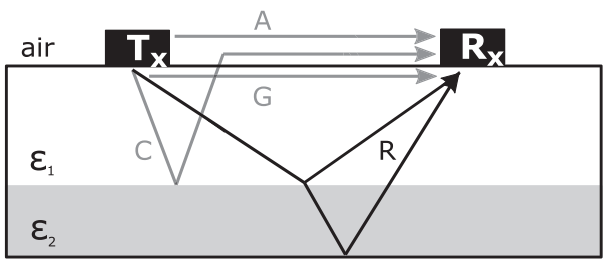

Fig. 1. Principle of GPR reflection and underlying signal paths between a transmitter T_x and a receiver R_x: A – direct air wave, G – direct ground wave, R – reflected wave, C – critical refracted wave (according to [16,25]).

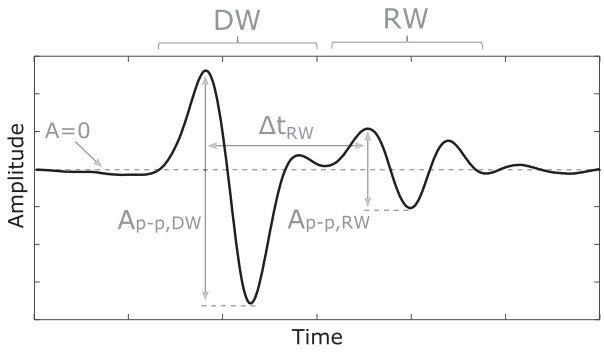

Fig. 2. Example of a recorded energy-signal in time domain (A-Scan) including the direct wave (DW) and reflection wave (RW). Basic signal features are the peak-to-peak amplitudes $A_{p-p,DW}$ and $A_{p-p,RW}$ located at the first peaks of DW and RW. The time difference Δt_{RW} between both peaks is often considered as the travel time.

The simplified ray-based wave paths describing these principles are shown in Fig. 1. The amount of reflected energy (R, black) of a transmitted pulse is dependent on the difference between the permittivities ε_1 and ε_2 of two considered materials. Expressed as a factor in the range of -1 and 1, the reflection coefficient r is calculated as follows:

$$r = \frac{\sqrt{\varepsilon_2} - \sqrt{\varepsilon_1}}{\sqrt{\varepsilon_2} + \sqrt{\varepsilon_1}} \tag{2}$$

Another important wave path is taken by the direct air (A, grey) and direct ground (G, grey) wave, which propagate in their respective medium on the shortest way between transmitter and receiver. With a small antenna spacing, both waves superpose and form the direct wave (DW) that is seen first in the received signal. A qualitative example of such a recorded energy-signal in time domain (A-Scan) is shown in Fig. 2. The DW is followed by a reflection wave (RW), with a certain peak-to-peak amplitude $A_{p-p,RW}$ and a time difference Δt_{RW} between DW and RW. These basic signal features, as well as the peak-to-peak amplitude of the DW, can already serve as good indicators for moisture measurements on building materials, which will be further discussed in Section 5. Similar to optics, refraction is described by Snell's law that deals with the relationship of occurring angles on interfaces. For reasons of clarity, the occurring refraction from ε_2 to ε_1 is not depicted in Fig. 1. Critical refractions and reflections (C, grey) also exist. They often superpose with the reflected wave R, which makes a separate investigation difficult. In general, the received A-Scan is always a superposition of all different wave paths, whereas their individual amplitude and separation in time and space depend on the spacing between transmitter and receiver as well as on the target depth and on the elevation of the antenna [31]. Different GPR configurations, therefore, have a considerable influence on the received signals and their interpretation. The commonly used set-ups for moisture measurements in building materials and their underlying parameters are discussed in the following section.

3. Configurations and their parameters

GPR configurations are divided into two types: reflection and transillumination measurements. Transillumination is rarely performed in civil engineering since a suitable back wall is often inaccessible (e.g tunnels, foundations, containments). Also, the transmission between a pair of boreholes, as it is applied by geophysicists for soil moisture measurements [24,34], is commonly not used to investigate building materials. This paper, therefore, focuses on reflection configurations. Here, the common–offset reflection survey, as shown in Fig. 3, is the simplest and mostly applied configuration. As the name of the method suggests, the spacing s between a single transmitter and a receiver is kept constant for every measurement position on a survey line. The most significant parameter is the applied center frequency, which describes the dominant frequency of the transmitted broadband pulse. As mentioned in Section 2, it influences the general attenuation and, therefore, the penetration depth. When it comes to multilayered mediums or rebar localization, the spatial resolution becomes more relevant since it rises with shorter wavelengths. This creates a trade-off between resolution and penetration depth when choosing the most suitable center frequency. GPR frequencies used for material moisture measurements are mainly between 100 kHz and 10 GHz. In case of concrete, frequencies between 1 GHz to 3 GHz yield a good trade-off between spatial resolution and penetration depth. Other essential parameters are the antenna spacing s, the antenna orientation, the bit resolution, recording time window, sampling frequency, the distance between each measurement and the parallel line spacing (when performing more than one survey line) [24]. The suitable choice of these values highly depends on the particular test object and purpose.

When using GPR in reflection configuration, one rarely has precise information about the underlying layer depth. In that case, a profound water content estimation through the use of velocity data is impossible since the traveled distance is unknown. Here, multi-offset configurations like common-midpoint (CMP) and wide angle reflection and refraction (WARR), as shown in Fig. 4, can be used. While the CMP method uses a fixed midpoint with a stepwise increasing spacing between transmitter and receiver, WARR configurations often have one source at a constant location with multiple receivers in defined distances. WARR can also be performed by using a single receiver (or transmitter) that is moved further from the corresponding transmitter (or receiver) with every measurement. The series of reflection waves (B-Scan) collected by multi-offset techniques form a hyperbola from which velocity and layer depth can be estimated [35–37]. After that, the obtained vertical velocity model allows a layer specific permittivity estimation.

4. Moisture content of building materials

As discussed in Section 2, the permittivity of an investigated material heavily depends on the moisture content and, therefore,

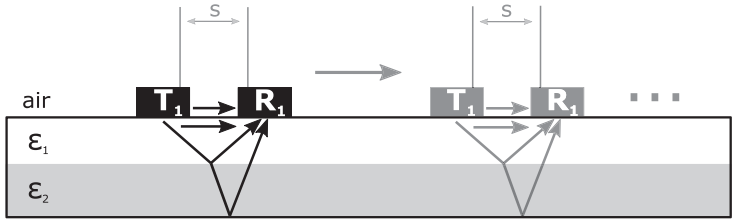

Fig. 3. Principle of a line measurement with GPR in common-offset configuration and its most important signal paths: Direct air wave, direct ground wave and the reflected waves.

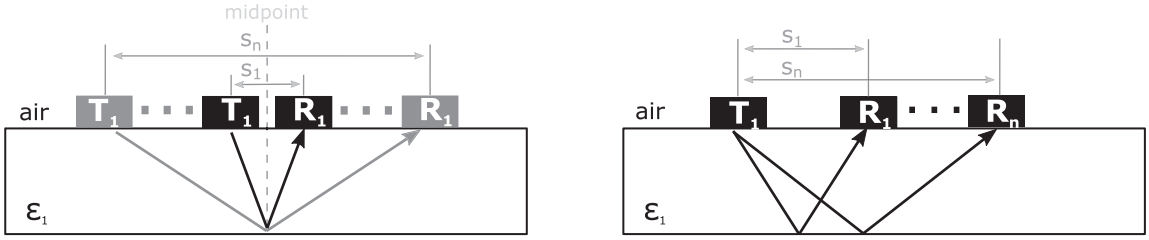

Fig. 4. GPR with multiple offsets: common-midpoint (CMP, left) and wide angle reflection and refraction (WARR, right) configuration.

changes when water is adsorbed. Water adsorption or desorption generally requires an open porosity as well as a hydrophobic behavior. Several building materials possess these material properties such as: concrete, screed, mineral rock wool, calcium silicate plate, etc. In these, the adsorbed water is located in completely filled pores and partially saturated pores [38].

Concrete is a highly heterogeneous material. Every concrete mixture has its own composition of water, cement, minerals, aggregates, additives, etc. This defines the resulting material properties, e.g. comprehensive strength, the dry density, and resistance to water and chlorides. Furthermore, the resulting pore system is also influenced significantly by the concrete composition as well as by the ambient temperature and humidity. On the long-term, the pore system might vary due to carbonation, micro-cracking, and sulphate attack. Thus, every pore system and hence every concrete is unique, and a general calibration function does not exist. Furthermore, the properties of the pore water are not time constant. Chloride and sulphate ingress change the surface tension of water, which changes the moisture content as well as the relative permittivity. In conclusion, quantitative moisture measurements of concrete would require intensive calibration for all the influencing factors mentioned above. Also in case of assumed perfect dry concrete samples (all evaporable pore water is released), no uniform permittivity exists. Every cement mixture contains different amounts of chemically bound water, calcium, aluminum, iron, etc. which influence the final permittivity.

The open porosity varies between 5% and 25% in most cases. The pore sizes are distributed over several magnitudes and are described by a representative diameter. Micro-pore diameters are between 0.4 nm and 2 nm, so called meso-pores are in the range of 2 nm to 100 nm, and macro-pores range from 100 nm up to 100 μm [39]. In these pores, the material moisture is located in liquid phase at the pore surface/ fringe and in vapor phase in the pore center. Occurring transportation processes are a two-phase flow including both phases, vapour and liquid. The total porosity and the distribution of the different pore sizes determine the capability of adsorption and desorption of water. The function which relates the water vapour partial pressure, i.e. relative humidity and the resulting material moisture is the so-called sorption isotherm.

In most cases, the moisture content of concrete is between 0.15 M% and 10 M%. It is defined as the ratio between the mass of moisture divided by the mass of the dry material. Besides this definition, sometimes the moisture content is based on the mass of the wet material or the volumetric moisture content is given [40]. For comparison, these values must be converted to each other. In the following, we use the definition based on the mass of the dry material. Obviously, this requires the knowledge of the dry mass. One common approach is oven drying to evaporate the mobile water in the pores [41]. Depending on the sample size, this might take up to several days. If mass constant is reached, the sample is considered as dry and all evaporable/ mobile water is released. Nevertheless, the cement matrix still contains a lot of chemically bound water. This water is immobile and never contributes to the moisture transport [11]. However, if the oven temperature is too high, this chemically bound water is partially released as well, which leads to systematic deviations from the "true" moisture content. In practice, various drying temperatures are established for different materials (cement based, calcium-sulphate based, clay minerals, etc.) and different testing purposes. Therefore, we will emphasize to consider clearly the drying method and a suitable temperature (in case of oven drying) when using moisture content values for calibration.

5. Determination of material moisture based on GPR

After the reflected energy-signals are recorded (Fig. 2), there are two possible ways to estimate the underlying water content θ. The first is illustrated by the steps A and B in Fig. 5, where the θ-estimation is based on a preceding ε-estimation. This is an appropriate approach, since the electric permittivity ε strongly depends on the material moisture [42]. However, such two-step calculations may increase the risk of error accumulation and therefore, already require a precise determination of ε. With a known ε, petrophysical models derived from empirical studies can be applied to calculate $\theta(\varepsilon)$. Topp's equation [43] is the most commonly used model in geophysics to estimate soil moisture [16,17]. Therefore, it is also applied in civil engineering to derive θ of subgrades below pavement and railway structures [20,44,45]. It provides a basic polynomial approximation for $\theta(\varepsilon)$, which only regards the real part of ε. For asphalt mixes, Fernandes et al. [46] applied a modification of the complex refractive index model (CRIM) derived by Wang and Lytton [47] to estimate the moisture content. CRIM offers a more complex approach, which requires further knowledge about the volumetric fraction of different material components. An overview of various petrophysical models and further literature can be found in [48].

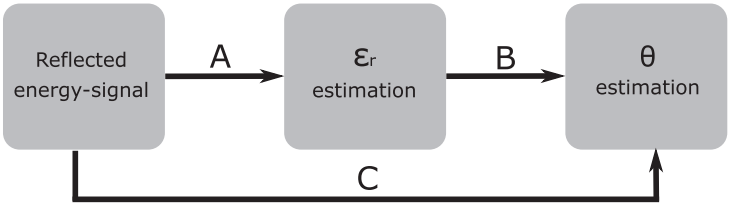

Fig. 5. Principle of signal processing to estimate the moisture content θ by using the reflected energy-signal of GPR.

When there is no established model for the investigated material, like for concrete, site-specific relationships based on the collected data serve as a suitable way to evaluate θ [49]. However, those fitted models always require an accurate reference of the underlying water contents. Here, the gravimetric method, as discussed in the previous section, provides results by drying and weighing collected samples (e.g. drilling cores) according to ASTM D2216-19 [41].

Such references also enable the second possible way to estimate θ, which is shown by step C in Fig. 5. This approach skips the ε-estimation by formulating a direct relationship between the received GPR signals and the obtained moisture data. Both approaches, AB and C, require characteristic signal features that correlate with θ. Those features commonly applied in civil engineering can be divided into time, amplitude, and frequency features. Their related methods and limitations will be discussed in the following sections.

5.1. Travel time and velocity features

Measuring the time Δt that it takes for a transmitted and reflected impulse to travel back to its origin is by far the oldest signal feature in radar technology [50]. It is generally used to detect objects and to calculate their distance d with Eq. 3 by means of the known wave velocity v.

$$v = \frac{2d}{\Delta t} \tag{3}$$

When performing moisture inspections with GPR, the permittivity of an investigated medium and hence the propagation velocity (Eq. 1) is obviously unknown. Therefore, a known reflector depth is one possibility to calculate v and ε by measuring Δt. It is usually performed in laboratory studies where the dimensions of test specimens are given, like in the works of Fernandes et al. [46], Lai et al. [22] and Laurens et al. [21]. Such set-ups allow an accurate determination of ε depending on the water content θ with a normal common–offset survey. This approach is also applicable to multilayered structures, as shown by Grote et al. [20]. Here, Δt is the time passing between two reflections from the top and bottom of a specific layer. In singlelayered mediums, Δt is often defined as the time difference between the first peak of the direct and the reflection wave (see Fig. 2), since the true time-zero is not available [51]. In the study of Viriyametanont et al. [52], the authors even propose a delay correction when using the direct wave as a time reference. This is motivated by a measurable influence of the underlying moisture content on the direct wave velocity, which can vary in near surface areas. The correction is calculated with a given transmitter to receiver offset and the wave velocity obtained from various rebar reflections in known depths.

In practice, usually the propagation velocity, as well as the reflector depth, are unknown. In this case, ASTM D6432-11 [37] suggests two techniques to obtain v from measured travel times. The first is called hyperbolic geometry and can be performed in common–offset configuration. It requires point reflectors such as pipes or rebars that cause a hyperbolic pattern in the radargram (B-Scan), from which the propagation velocity can be derived. Cheung and Lai [53] recently used this technique to detect water-pipe leakages by observing significant velocity drops compared to undamaged dry areas. A quantitative approach was studied by Koyan et al. [54] who presented a migration-based velocity analysis on multiple rebar reflections, however, this was done with known reflector depths to conduct a time-zero correction. Here, occurring uncertainties were mainly caused by interferences due to a small spacing between the rebars and a limited vertical resolution for shallow rebar depths.

The second way to obtain v without a known d is called velocity sounding which describes the use of the CMP or WARR survey method, as mentioned in Section 3. CMP measurements were applied by Cai et al. [45] and Grote et al. [20] to obtain a vertical velocity characterization for railway and pavement structures, respectively. The use of such multi-offset configurations also allows greater spacing between transmitter and receiver. Therefore, the travel time of the direct wave gets more relevant while it is barely considered in common–offset configuration. Klysz and Balayssac [19] suggest the analysis of direct wave travel times with WARR configuration to estimate the mositure content of concrete covers. However, it is important to mention that only near surface moisture can be measured with this technique, since the penetration depth of the ground wave is limited [55].

5.2. Amplitude and attenuation features

Quantitative estimation of underlying permittivities by analyzing the received signal amplitudes is very challenging compared to the use of travel times [20]. The theoretical approach is given with Eq. 2, which suggests the evaluation of occurring reflections on a boundary of two different permittivities. Besides the need of one given ε, this method often leads to inaccuracies due to several other influences on the amplitude. In complex mediums, like concrete, the propagating waves experience a lot of scattering through heterogeneously distributed electrical properties [25]. An increased moisture content leads to the presence of more water filled pores and thus to more heterogeneities and a higher conductivity. Furthermore, attenuation grows with longer travel paths and rising frequencies, which distorts an amplitude-based ε-estimation even more.

The use of an air-launched and, therefore, air-coupled antenna configuration makes it possible to analyze the reflection that occurs on the air-material interface. Air, as the overlying medium, has a known permittivity $\varepsilon_{air} = 1$ and causes comparatively low losses. Thus, the permittivity of the underlying material ε_m can be calculated with the following equation:

$$\varepsilon_m = \left[\frac{1 + \frac{A_0}{A_m}}{1 - \frac{A_0}{A_m}}\right]^2 \tag{4}$$

Here, the reflection coefficient is defined as $r = A_0/A_m$ with the reflected air-surface amplitude A_0, that is scaled by the highest possible amplitude A_m. This maximum can be easily obtained with the use of a metallic reflector in the same distance as the investigated surface. Benedetto et al. [44] used this technique to map the spatial variation of soil moisture as a preinvestigation for pavement applications. However, this approach only covers moisture near the surface and ignores possible permittivity changes in deeper areas. To capture those, Maser and Scullion [56] also analyzed the reflections from the asphalt-bottom to estimate the moisture content of the underlying base layer. Obviously, this method encounters all the aforementioned uncertainties with the additional risk of error accumulation by the use of previously estimated asphalt permittivities.

Due to the numerous unknown influences for on site investigations, most of the works that study the correlation between amplitudes and water content were performed under laboratory conditions. A controlled environment also allows the use of additional metallic reflectors below the investigated specimens to emphasize the occurring reflections or to generate reference amplitudes for scaling/ normalization. As a signal feature, Hugenschmidt and Loser [57] used the quotient between the reflected amplitudes at the concrete surface and those at an aluminum sheet below the bottom. The authors observed a qualitative correlation with the water content of concrete as well as with ingressed chlorides that increase the underlying conductivity and therefore cause

additional attenuation. This is particularly an issue in countries where salt is used for de-icing roads and pavements. The concurrent influence of moisture and chlorides in concrete was also studied by Senin and Hamid [58]. It was observed that ingressed chlorides attenuate the amplitude even more with rising water contents, which is explained by a rising mobility of the chloride ions in water filled pores. To obtain a signal feature, the authors defined an amplitude attenuation per meter with known sample thicknesses. Here, the received amplitude of a completely dry and chloride free reference-sample served as the normalizing factor. Lai et al. [22] used a similar attenuation feature expressed in dB/m to observe the hydration process of concrete. The authors normalized the reflection-amplitudes with those of the direct wave. This may lead to errors since the amplitude of the direct wave is also sensitive to the underlying moisture content, as shown in the works of Klysz and Balayssac [19] and Sbartai et al. [59]. The latter took the amplitude of the direct wave in air as the nomalizing factor to ensure a material-independent reference. Another possibility to scale received amplitudes is shown by Laurens et al. [21] who use the reflection of a fully saturated specimen to emphasize the contrast of different moisture contents.

In Klee and Kind [60], the authors presented a statistical approach in which they analyzed the root mean square (RMS) of time-slices (C-Scans) during the hydration process of concrete. The general procedure is described in Kind et al. [61]. C-Scans can be obtained by measuring more than one survey line with a parallel spacing to each other, which generates a data cube (e.g. in the work of Weise et al. [62]). A horizontal slice out of that data cube includes all samples (amplitudes) for a certain time value of all recorded reflection signals. During hydration, the RMS significantly rose in the time range of the back wall reflections, but did not show any remarkable changes for other time ranges.

In most cases outside the laboratory, practical studies only allow qualitative statements on moisture contents. An example is the work of Alani et al. [63], where the general signal attenuation served as a suitable indicator for specific bridge areas affected by moisture ingress.

5.3. Features in the frequency domain

In comparison to the classical features like amplitude and travel time, represented by specific points in time domain, frequency related features include the information of certain time ranges or the complete time signal. Extracting these features makes it possible to observe a shift to lower frequencies in the received waveforms with rising water contents [21].

One way to explain this phenomenon is the occurrence of Rayleigh scattering [30]. It describes the scattering on heterogeneities that are much smaller in size than the applied wavelength of the electromagnetic wave [25]. As mentioned before, higher water contents go along with a higher number of water filled pores. The additional heterogeneities attenuate higher frequencies even more which results in the observable shift. To capture this dependency, Benedetto and Tedeschi [64] compare the peak frequencies of different spectra obtained by fast fourier tranformation (FFT) to indicate qualitative changes in the water content. In addition to that, the authors extract the spectrum's second, third, and fourth standardized moments, which represent the variance, skewness and kurtosis, respectively. However, the use of higher order statistics requires a larger sample size to maintain the same level of accuracy, which is discussed in [65].

Another explanation for the frequency shift is dielectric dispersion, which describes the frequency dependent behavior of ε. As stated in Section 2, free water has a relaxation frequency between 10 and 20 GHz, which marks the highest possible imaginary part of ε and thus the highest frequency dependent attenuation. For composite materials with bound water, like soil or concrete, the relaxation frequency is significantly smaller compared to free water [66]. The influence of free and bound water on the frequencies of an reflected signal was studied by Lai et al. [67] on hydrating concrete samples. By using the short-time Fourier transformation (STFT), it was shown that the higher frequency components of the reflection wave get less attenuated with a rising share of bound water, which can be explained with the increased inertia of bound molecules [48]. The use of STFT, as a joint time–frequency analysis, makes it possible to analyze the spectra of different time steps in the received signal. Thus, occurring changes for different wave types like the direct and reflected wave are detectable, as their occurrence is separated in time. In comparison, the fast fourier transformation (FFT) analyzes the entire signal only, which may lead to a lower sensitivity for spectral shifts in specific time ranges.

In Lai et al. [68] the authors used the STFT to qualitatively observe the drying of a brick wall by evaluating the spectral shift of the direct wave. The same data was later analyzed with the wavelet transformation (WT), which is presented in Lai et al. [69]. Compared to the fixed time–frequency resolution of the STFT, the WT offers varying resolution characteristics. This results in a more accurate analysis of both lower and higher frequency components with a decreasing time resolution for lower and an increasing time resolution for higher frequencies. For the direct and reflection wave, the drying process becomes more detectable with the use of WT compared to the application of STFT.

All mentioned publications concerning variations in the frequency spectra present a qualitative approach since the theoretical influences are not completely understood. Nevertheless, frequency features can serve as an appropriate addition to previously mentioned techniques.

The discussed publications that used an amplitude, time, or frequency feature to detect moisture in the context of civil engineering are listed in Table 1.

5.4. Inversion-based methods

The available computing power motivates sophisticated approaches, like full-waveform inversion, that include the accurate modeling of electromagnetic wave propagation [71]. The idea is to incrementally change the unknown model parameters (permittivity ε and conductivity σ) until the misfit between synthetic and collected data is minimized. Hence, a precise model of the applied GPR system and the underlying medium is of high importance to ensure appropriate results. In addition to increasing applications for geophysical studies using GPR [72], full-waveform inversion is also used to assess moisture and chlorides in concrete [73,74].

Another inversion-based approach evaluates the occurring dispersion caused by thin low-velocity layers that act as waveguides [75–77]. Xiao et al. recently applied this principle to monitor the water ingress and transfer in concrete [78,79].

The inversion-based methods show promising results, however they are still considered as advanced research, that requires skilled and experienced users [80]. As a tool for modeling synthetic data, open source simulation software like GprMax [81] can be used.

5.5. Problems and limitations of on site investigations

Numerous works in this review where performed in laboratory conditions, where the authors are able to measure and control crucial parameters. Knowledge about the thickness of objects, the material composition, a uniform water distribution, available reference measurements from dry states or the surrounding temperature and humidity are necessary for a reliable quantification of moisture contents. While these works reveal important information and experience about the application of GPR, their transfer

Table 1
Overview of publications that perform moisture measurements in civil engineering based on signal features of the radar signal. DW - direct wave; RW - reflection wave; CO(al) - common-offset (air-launched); A, B, C – according to Fig. 5; f_c – applied center frequency.

Reference	Signal Feature	Signal Part	Survey Method	Estimation Method	f_c [GHz]
Alani et al. [63]	Amplitude	DW, RW	CO	Qualitative	2
Benedetto et al. [44]	Amplitude Frequency	RW, A-Scan	CO(al)	A, B (Topp)	0.6, 1.6
Benedetto and Tedeschi [64]	Frequency	A-Scan	CO	Qualitative	0.6, 1.6
Cai et al. [45]	Time	RW	CMP	A, B (Topp)	0.1
Cheung and Lai [53]	Time	RW	CO	Qualitative	0.2, 0.25, 0.4, 0.6, 0.9
Fernandes et al. [46]	Time	RW	CO	A, B (Wang)	1.6
Grote et al. [20]	Amplitude Time	DW, RW	CO, CMP	A, B (Topp and site-specific)	0.9, 1.2
Hugenschmidt and Loser [57]	Amplitude	RW	CO(al)	Qualitative	2.5
Klee and Kind [60]	Amplitude	C-Scan	CO	Qualitative	1.5, 2.6
Klysz and Balayssac [19]	Amplitude Time	DW, RW	CO, WARR	C	1.5
Koyan et al. [54]	Time	RW	CO	A, B (CRIM)	2
Lai et al. [22]	Amplitude Time	DW, RW	CO	A	1
Lai et al. [67–69]	Frequency	A-Scan	CO	Qualitative	1.5, 2.6
Laurens et al. [21]	Amplitude Time Frequency	DW, RW	CO	A, C	1.5
Maser and Scullion [56]	Amplitude	RW	CO(al)	A, B (CRIM)	1
Senin and Hamid [58]	Amplitude	DW, RW	CO	C	1.6
Sbartai et al. [59]	Amplitude	DW, RW	CO	C	1.5
Viriyametanont et al. [52]	Time	RW	CO	A	1.5
Weise et al. [62]	Time	RW	CO	Qualitative	2.6

to a practical on site investigation is not straightforward. Here, most of or even all of the aforementioned parameters are initially unknown. Thus, we want to emphasize that on site investigations should always be performed or supervised by trained personnel who is familiar with the difficulties between laboratory and field tests.

One of the most common reasons for misinterpretation is an imprecise assumption of the actual wave travel path, since it provides the basis for an accurate velocity analysis as discussed in Section 5.1 and influences received amplitudes as well. Extracting drilling cores or perform bigger excavations are direct ways to overcome this problem, like shown in the works of Alani et al. [63], Maser and Scullion [56] and Weise et al. [62]. However, these inspections often can only be done selectively, whereby some thickness variations may remain unnoticed. Here, former collected reference measurements from dry states can provide precise information [20], which generally justifies long term monitoring of certain objects that might constitute a risk to security like roads and bridges. CMP measurements performed in the works of Cai et al. [45] and Grote et al. [20] also deal with the problem of unknown object thicknesses. However, interference between certain wave parts or reflections due to shallow structures might lead to errors. Cai et al. [45] performed simulations with GprMax to identify advantageous trace ranges for their calculations. Furthermore, the choice of a more suitable center frequency may provide better resolution in such cases.

Besides unknown wave travel paths, changing material properties caused by e.g. density or moisture gradients can also cause misinterpretations, since the applied calculations often assume uniform distributions. Here again, the extraction of drilling cores can give good insights into such variations.

Apart from verifying structural properties like the material thickness or composition, indicating the presence of water with other methods like capacitive probes [44] or the use of nuclear magnetic resonance (NMR) [62] may support the correct interpretation of GPR data. Sometimes, even the visual inspection of small surface cracks that serve as ingress ways for moisture [63] or darker areas of a concrete road [62] provide significant hints.

The amount of unknown parameters when performing on site measurements with GPR underlines the general need of trained and experienced personnel. A comprehensive knowledge about the influence of moisture on the various signal features as well as a detailed assessment of possible errors is necessary to achieve meaningful results.

6. Summary and conclusion

In this work, we presented an overview of applied methods to perform moisture measurements with GPR in the context of civil engineering. It focused especially on the variety of used signal features in the reflected energy signal as well as on the respective survey methods and the differing approaches to estimate θ.

While the quantitative determination of underlying water contents already delivers good results in laboratory conditions, users have to deal with a lot of uncertainties when it comes to on site investigations. Unknown underlying component dimensions or material properties can easily lead to misinterpretations as they may have a significant influence on the applied signal features. Therefore, destructive methods like the analysis of drilling cores are often necessary to obtain the missing information or to calibrate collected data. However, the knowledge about the presented methods and signal features, as well as their limitations, can already provide a good basis for qualitative on site assessments of moisture ingress and damage.

Future works should investigate the combination of different signal features or methods, as it is remarkable that most of the studies either focused on a single feature or analyzed a number of them separately. An advanced approach is already given with the emerging inversion-based methods, that even consider the entire waveform and include the conductivity as an additional model parameter. Furthermore, combining different features with the use of data fusion and machine learning may also drive progress towards automation. However, such approaches require a representative data basis, which is usually not available. The trend towards open data could close this gap and encourage further studies on the suitability of learning-based strategies.

Declaration of Competing Interest

The authors declare that they have no known competing financial interests or personal relationships that could have appeared to influence the work reported in this paper.

Acknowledgments

This work was funded by the Bundesanstalt für Materialforschung und -prüfung. Additionally, the authors would like to thank Thomas Kind and Christian Köpp for their helpful comments on the text.

References

[1] Y. Zhang, G. Ye, A model for predicting the relative chloride diffusion coefficient in unsaturated cementitious materials, Cem. Concr. Res. 115 (2019) 133–144.
[2] A. Bentur, N. Berke, S. Diamond, Steel corrosion in concrete: fundamentals and civil engineering practice, CRC Press, 1997.
[3] D.W. Hobbs, Alkali-silica reaction in concrete, Thomas Telford Publishing, 1988.
[4] K.F. Nielsen, G. Holm, L.P. Uttrup, P.A. Nielsen, Mould growth on building materials under low water activities, Influence of humidity and temperature on fungal growth and secondary metabolism, Int. Biodeterioration Biodegradation 54 (2004) 325–336, https://doi.org/10.1016/j.ibiod.2004.05.002.
[5] S. Jacobsen, J. Marchand, L. Boisvert, Effect of cracking and healing on chloride transport in OPC concrete, Cem. Concr. Res. 26 (1996) 869–881, https://doi.org/10.1016/0008-8846(96)00072-5.
[6] C. Dow, F.P. Glasser, Calcium carbonate efflorescence on Portland cement and building materials, Cem. Concr. Res. 33 (2003) 147–154, https://doi.org/10.1016/S0008-8846(02)00937-7.
[7] L. Pel, K. Kopinga, H. Brocken, Moisture transport in porous building materials, Technische Universiteit Eindhoven, 1995 (Ph.D. thesis).
[8] J. MacGregor, J.K. Wight, S. Teng, P. Irawan, Reinforced concrete: Mechanics and design, vol. 3, Prentice Hall Upper Saddle River, NJ, 1997.
[9] GDV, Annual of Gesamtverband der Deutschen Versicherungswirtschaft e.V., https://www.gdv.de/de/zahlen-und-fakten/versicherungsbereiche/wohngebaeude-24080, 2018. Accessed on 11/07/2019.
[10] S. Kruschwitz, Feuchtemessung im Bauwesen - ein Überblick, Fachtagung Bauwerksdiagnose, Vortrag 5 (2014).
[11] L.-O. Nilsson (Ed.), Methods of Measuring Moisture in Building Materials and Structures, Springer International Publishing, 2018.
[12] M.I. Skolnik, An introduction to radar, Radar handbook 2 (1962) 1–21.
[13] D. Atlas, Radar in Meteorology: Battan Memorial and 40th Anniversary Radar Meteorology Conference, Springer, 2015.
[14] M. Schneider, Automotive radar-status and trends, in: German microwave conference, pp. 144–147.
[15] R. Orosei, S.E. Lauro, E. Pettinelli, A. Cicchetti, M. Coradini, B. Cosciotti, F.D. Paolo, E. Flamini, E. Mattei, M. Pajola, F. Soldovieri, M. Cartacci, F. Cassenti, A. Frigeri, S. Giuppi, R. Martufi, A. Masdea, G. Mitri, C. Nenna, R. Noschese, M. Restano, R. Seu, Radar evidence of subglacial liquid water on Mars, Science (2018) eaar7268, https://doi.org/10.1126/science.aar7268.
[16] J.A. Huisman, S.S. Hubbard, J.D. Redman, A.P. Annan, Measuring soil water content with ground penetrating radar: a review, Vadose Zone J. 2 (2003) 476–491, https://doi.org/10.2113/2.4.476.
[17] L. Slater, X. Comas, The Contribution of Ground Penetrating Radar to Water Resource Research, in: Ground Penetrating Radar: Theory and Applications, Elsevier, 2009.
[18] T. Saarenketo, T. Scullion, Road evaluation with ground penetrating radar, J. Appl. Geophys. 43 (2000) 119–138, https://doi.org/10.1016/s0926-9851(99)00052-x.
[19] G. Klysz, J.-P. Balayssac, Determination of volumetric water content of concrete using ground-penetrating radar, Cem. Concr. Res. 37 (2007) 1164–1171, https://doi.org/10.1016/j.cemconres.2007.04.010.
[20] K. Grote, S. Hubbard, J. Harvey, Y. Rubin, Evaluation of infiltration in layered pavements using surface GPR reflection techniques, J. Appl. Geophys. 57 (57) (2005) 129–153, https://doi.org/10.1016/j.jappgeo.2004.10.002.
[21] S. Laurens, J.P. Balayssac, J. Rhazi, G. Klysz, G. Arliguie, Non-destructive evaluation of concrete moisture by GPR: experimental study and direct modeling, Mater. Struct. 38 (38) (2005) 827–832, https://doi.org/10.1007/BF02481655.
[22] W.L. Lai, S.C. Kou, W.F. Tsang, C.S. Poon, Characterization of concrete properties from dielectric properties using ground penetrating radar, Cem. Concr. Res. 39 (2009) 687–695, https://doi.org/10.1016/j.cemconres.2009.05.004.
[23] J.C. Maxwell, A dynamical theory of the electromagnetic field, Philos. Trans. R. Soc. Lond. 155 (1865) 459–512, https://doi.org/10.1098/rstl.1865.0008.
[24] A.P. Annan, GPR methods for hydrogeological studies, in: Hydrogeophysics, Springer, 2005, pp. 185–213, https://doi.org/10.1007/1-4020-3102-5.
[25] A.P. Annan, Electromagnetic Principles of Ground Penetrating Radar, in: H.M. Jol (Ed.), Ground Penetrating Radar: Theory and Applications, Elsevier, 2009, pp. 4–38.
[26] D.J. Daniels, Ground Penetrating Radar, second ed., The Institution of Engineering and Technology, 2007.
[27] U. Kaatze, Complex permittivity of water as a function of frequency and temperature, J. Chem. Eng. Data 34 (1989) 371–374, https://doi.org/10.1021/je00058a001.
[28] P.J.W. Debye, Polar molecules, The Chemical Catalog Company Inc, New York, 1929.
[29] K.S. Cole, R.H. Cole, Dispersion and Absorption in Dielectrics I. Alternating Current Characteristics, J. Chem. Phys. 9 (1941) 341–351.
[30] C. Bohren, D. Huffman, Absorption and Scattering of Light by Small Particles, Wiley, 1983.
[31] A.P. Annan, Ground Penetrating Radar Principles, Procedures & Applications, Technical Report, Sensors & Software Inc., 2003.
[32] M.N. Soutsos, J.H. Bungey, S.G. Millard, M.R. Shaw, A. Patterson, Dielectric properties of concrete and their influence on radar testing, NDT&E Int. 34 (2001) 419–425, https://doi.org/10.1016/S0963-8695(01)00009-3.
[33] S. Okamura, Microwave technology for moisture measurement, Subsurf. Sens. Technol. Appl. 1 (2000) 205–227.
[34] E.W. Gilson, J.D. Redman, J. Pilon, A.P. Annan, Near Surface Applications of Borehole Radar, Symposium on the Application of Geophysics to Engineering and Environmental Problems (1996), https://doi.org/10.4133/1.2922317.
[35] C.H. Dix, Seismic velocities from surface measurements, Geophysics 20 (1955) 68–86.
[36] J. Hugenschmidt, Multi-offset analysis for man-made structures, in: 8th International Conference on Ground Penetrating Radar, 2000.
[37] ASTM D6432-11, Standard Guide for Using the Surface Ground Penetrating Radar Method for Subsurface Investigation, ASTM 04 (2011) 09.
[38] C. Strangfeld, S. Kruschwitz, Monitoring of the absolute water content in porous materials based on embedded humidity sensors, Constr. Build. Mater. 177 (2018) 511–521, https://doi.org/10.1016/j.conbuildmat.2018.05.044.
[39] ISO, ISO 15901-2:2006(E): Pore size distribution and porosity of solid materials by mercury porosimetry and gas adsorption – Part 2: Analysis of mesopores and macropores by gas adsorption, International Standard, 2006.
[40] U. Kaatze, C. Hübner, Electromagnetic techniques for moisture content determination of materials, Meas. Sci. Technol. 21 (2010), https://doi.org/10.1088/0957-0233/21/8/082001 082001.
[41] ASTM D2216-19, Standard Test Methods for Laboratory Determination of Water (Moisture) Content of Soil and Rock by Mass, ASTM 04 (2019) 08.
[42] J.L. Davis, A.P. Annan, Electromagnetic detection of soil moisture: progress report I, Can. J. Remote Sens. 3 (1977) 76–86, https://doi.org/10.1080/07038992.1977.10854959.
[43] G.C. Topp, J.L. Davis, A.P. Annan, Electromagnetic determination of soil water content: measurements in coaxial transmission lines, Water Resour. Res. 16 (1980) 574–582, https://doi.org/10.1029/WR016i003p00574.
[44] A. Benedetto, F. Tosti, B. Ortuani, M. Giudici, M. Mele, Soil moisture mapping using GPR for pavement applications, Penetrating Radar, 2013, https://doi.org/10.1109/iwagpr.2013.6601550.
[45] J.Q. Cai, S.X. Liu, L. Fu, Y.Q. Feng, Detection of railway subgrade moisture content by GPR, in: 16th International Conference on Ground Penetrating Radar (GPR), 2016, https://doi.org/10.1109/ICGPR.2016.7572613.
[46] F.M. Fernandes, A. Fernandes, J. Pais, Assessment of the density and moisture content of asphalt mixtures of road pavements, Constr. Build. Mater. 154 (2017) 1216–1225, https://doi.org/10.1016/j.conbuildmat.2017.06.119.
[47] F. Wang, R.L. Lytton, System identification method for backcalculating pavement layer properties, Transp. Res. Rec. 1384 (1993).
[48] N.J. Cassidy, Electrical and Magnetic Properties of Rocks, Soils and Fluids, in: Ground Penetrating Radar: Theory and Applications, Elsevier, 2009, pp. 41–72, https://doi.org/10.1016/B978-0-444-53348-7.00002-8.
[49] C. Chen, J. Zhang, A Review on GPR Applications in Moisture Content Determination and Pavement Condition Assessment, GeoHunan International Conference (2009), https://doi.org/10.1061/41041(348)20.
[50] C. Hülsmeyer, Patent DE169154: Verfahren zur Bestimmung der Entfernung von metallischen Gegenständen (Schiffen o. dgl.), deren Gegenwart durch das Verfahren nach Patent 165546 festgestellt wird, Patent claimed 11/11/1904, published 04/02/1996 (1904).
[51] R. Yelf, Where is true time zero?, in: Proceedings of the Tenth International Conference on Ground Penetrating Radar, 2004, https://doiorg/10.1109/ICGPR.2004.179979.
[52] K. Viriyametanont, S. Laurens, G. Klysz, J.-P. Balayssac, G. Arliguie, Radar survey of concrete elements: effect of concrete properties on propagation velocity and time zero, NDT&E Int. 41 (2008) 198–207, https://doi.org/10.1016/j.ndteint.2007.10.001.
[53] B.W.-Y. Cheung, W.W.-L. Lai, Field validation of water-pipe leakage detection through spatial and time-lapse analysis of GPR wave velocity, Near Surface Geophys. 17 (2019) 231–246, https://doi.org/10.1002/nsg.12041.
[54] P. Koyan, J. Tronicke, N. Allroggen, A. Kathage, M. Willmes, Estimating moisture changes in concrete using GPR velocity analysis: potential and limitations, in: 17th International Conference on Ground Penetrating Radar (GPR), 2018, https://doi.org/10.1109/ICGPR.2018.8441572.
[55] K. Grote, T. Crist, C. Nickel, Experimental estimation of the GPR groundwave sampling depth, Water Resour. Res. 46 (2010), https://doi.org/10.1029/2009WR008403.
[56] K.R. Maser, T. Scullion, Automated pavement subsurface profiling using radar: case studies of four experimental field sites, Transp. Res. Rec. 1344 (1991) 148–154.
[57] J. Hugenschmidt, R. Loser, Detection of chlorides and moisture in concrete structures with ground penetrating radar, Mater. Struct. 41 (2008) 785–792, https://doi.org/10.1617/s11527-007-9282-5.
[58] S.F. Senin, R. Hamid, Ground penetrating radar wave attenuation models for estimation of moisture and chloride content in concrete slab, Constr. Build. Mater. 106 (2016) 659–669, https://doi.org/10.1016/j.conbuildmat.2015.12.156.
[59] Z.M. Sbartai, S. Laurens, J.-P. Balayssac, G. Ballivy, G. Arliguie, Effect of concrete moisture on radar signal amplitude, ACI Mater. J. (2006).
[60] M. Klee, T. Kind, Untersuchung des Einflusses von Hydratisierung und Feuchte auf die Radarstreuung an der Heterogenität von Beton, 77, Jahrestagung der DGG (2017).
[61] T. Kind, C. Trela, M. Schubert, J. Wostmann, Aggregates scattering of GPR waves in concrete, in: Proceedings of the 15th International Conference on Ground Penetrating Radar, 2014, https://doi.org/10.1109/ICGPR.2014.6970557.

[62] F. Weise, T. Kind, L. Stelzner, M. Wieland, Dunkelfärbung der betonfahrbahndecke im AKR-kontext, Beton- und Stahlbetonbau 113 (2018) 647–655, https://doi.org/10.1002/best.201800020.
[63] A.M. Alani, M. Aboutalebi, G. Kilic, Applications of ground penetrating radar (GPR) in bridge deck monitoring and assessment, J. Appl. Geophys. 97 (2013) 45–54, https://doi.org/10.1016/j.jappgeo.2013.04.009.
[64] F. Benedetto, A. Tedeschi, Moisture content evaluation for road-surfaces monitoring by GPR image and data processing on mobile platforms, in: 3rd International Conference on Future Internet of Things and Cloud, 2015, pp. 602–607, https://doi.org/10.1109/FiCloud.2015.44.
[65] A. Benedetto, F. Benedetto, Remote Sensing of Soil Moisture Content by GPR Signal Processing inf the Frequency Domain, IEEE Sens. J. 11 (2011) 2432–2441, https://doi.org/10.1109/JSEN.2011.2119478.
[66] T. Saarenketo, Electrical properties of water in clay and silty soils, J. Appl. Geophys. 40 (1998) 73–88, https://doi.org/10.1016/S0926-9851(98)00017-2.
[67] W.L. Lai, T. Kind, H. Wiggenhauser, A study of concrete hydration and dielectric relaxation mechanism using ground penetrating radar and short-time fourier transform, EURASIP J. Adv. Signal Process. 2010 (2010), https://doi.org/10.1155/2010/317216.
[68] W.L. Lai, T. Kind, H. Wiggenhauser, Using ground penetrating radar and time–frequency analysis to characterize construction materials, NDT & E Int. 44 (2011) 111–120, https://doi.org/10.1016/j.ndteint.2010.10.002.
[69] W.L. Lai, T. Kind, S. Kruschwitz, J. Wöstmann, H. Wiggenhauser, Spectral absorption of spatial and temporal ground penetrating radar signals by water in construction materials, NDT & E Int. 67 (2014) 55–63, https://doi.org/10.1016/j.ndteint.2014.06.009.
[71] S. Busch, J. van der Kruk, J. Bikowski, H. Vereecken, Quantitative conductivity and permittivity estimation using full-waveform inversion of on-gorund GPR data, Geophysics 77 (2012) H79–H91, https://doi.org/10.1190/geo2012-0045.1.
[72] A. Klotzsche, F. Jonard, M.C. Looms, J. van der Kruk, J.A. Huisman, Measuring soil water content with ground penetrating radar: a decade of progress, Vadose Zone J. 17 (2018), https://doi.org/10.2136/vzj2018.03.0052 180052.
[73] A. Kalogeropoulos, J. van der Kruk, J. Hugenschmidt, S. Busch, K. Merz, Chlorides and moisture assessment in concrete by GPR full waveform inversion, Near Surface Geophys. 9 (2011) 277–286, https://doi.org/10.3997/1873-0604.2010064.
[74] A. Kalogeropoulos, J. van der Kruk, J. Hugenschmidt, J. Bikowski, E. Brühwiler, Full-waveform GPR inversion to assess chloride gradients in concrete, NDT&E Int. 57 (2013) 74–84, https://doi.org/10.1016/j.ndteint.2013.03.003.
[75] J. van der Kruk, Properties of surface waveguides derived from inversion of fundamental and higher mode dispersive GPR data, IEEE Trans. Geosci. Remote Sens. 44 (2006) 2908–2915, https://doi.org/10.1109/TGRS.2006.877286.
[76] J. van der Kruk, S.A. Arcone, L. Liu, Fundamental and higher mode inversion of dispersed GPR waves propagating in an ice layer, IEEE Trans. Geosci. Remote Sens. 45 (2007) 2483–2491, https://doi.org/10.1109/TGRS.2007.900685.
[77] J. van der Kruk, R.W. Jacob, H. Vereecken, Properties of precipitation-induced multilayer surface waveguides derived from inversion of dispersive TE and TM GPR data, Geophysics 75 (2010) WA263–WA273, https://doi.org/10.1190/1.3467444.
[78] X. Xiao, A. Ihamouten, G. Villain, X. Dérobert, Use of electromagnetic two-layer wave-guided propagation in the GPR frequency range to characterize water transfer in concrete, NDT&E Int. 86 (2017) 164–174, https://doi.org/10.1016/j.ndteint.2016.08.001.
[79] X. Xiao, A. Ihamouten, G. Villain, X. Derobert, G. Tian, Modeling of Water Contents in Concrete Using Electromagnetic Guided Waves, Transactions of Nanjing University of Aeronautics and Astronautics, 2017.
[80] W.W.-L. Lai, X. Dérobert, P. Annan, A review of ground penetrating radar application in civil engineering: a 30-year journey from locating and testing to imaging and diagnosis, NDT&E Int. 96 (2018) 58–78, https://doi.org/10.1016/j.ndteint.2017.04.002.
[81] C. Warren, A. Giannopoulos, I. Giannakis, gprMax: open source software to simulate electromagnetic wave propagation for ground penetrating radar, Comput. Phys. Commun. 209 (2016) 163–170, https://doi.org/10.1016/j.cpc.2016.08.020.